Smart Structures and Systems, *Vol. 33, No. 6 (2024) 385-398*
https://doi.org/10.12989/sss.2024.33.6.385

A new time-frequency analysis and structural instantaneous frequency extraction method based on modified spline-kernelled chirplet transform

Dong-Yan Xue [1a], Ping-Ping Yuan[*1], Zhou-Jie Zhao [1b] and Wei-Xin Ren [2c]

[1] *School of Civil Engineering and Architecture, Jiangsu University of Science and Technology, Zhenjiang, 212100, Jiangsu, China*
[2] *College of Civil and Transportation Engineering, Shenzhen University, Shenzhen, 518060, Guangdong, China*

(*Received May 31, 2023, Revised April 24, 2024, Accepted June 12, 2024*)

Abstract. To improve the accuracy of time-frequency analysis (TFA) and instantaneous frequency (IF) extraction of structural dynamic response signals, this paper improves the spline-kernelled chirplet transform, and a new form of modified spline-kernelled chirplet transform (MSCT) based on revised Gaussian window function and energy concentration principle is put forward. The effectiveness of the proposed method is verified by numerical examples of single-component signal, multi-component signal, single-degree-of-freedom Duffing nonlinear system and two-layer shear frame structure model. Then, a time-varying cable test is designed to collect the acceleration response signals under linear changing tension, and the IF extraction of these signals is performed by using MSCT, which further verifies the effectiveness and accuracy of this method. Through numerical simulation and experimental verification, it is proved that the proposed method can effectively extract the IF of nonlinear structure and time-varying structure.

Keywords: instantaneous frequency (IF); modified spline-kernelled chirplet transform (MSCT); parameter optimization; time-frequency analysis (TFA); time-varying signal

1. Introduction

In the field of signal analysis, traditional Fourier transform can only be used to analyze stationary signals, but in practical engineering, the signal response has non-stationary and nonlinear characteristics in the face of various complex loads. The TFA method can extract instantaneous features of signals in both the time and frequency domains, which is a powerful tool for analyzing non-stationary signals (Yan *et al*. 2015, Pang *et al*. 2014). The commonly used TFA methods include short-time Fourier transform (STFT), Wigner-Ville distribution, Wavelet transform (WT), S-transform (ST) and so on (Zhang *et al*. 2014). However, inherent drawbacks always lie in these classical TFA techniques. For example, the width of each window function in STFT is constant, which leads to its poor ability in analyzing non-stationary signals with rapidly-changing IFs (Zhu *et al*. 2019a). The bilinear transform of the Winger-Ville distribution makes it difficult to suppress its cross-interference term, which can generate false frequencies (Li and Crocker 2006, Djurović and Stankovic 2004). WT is a Fourier transform with adjustable window, but it has the problem of fuzzy time-frequency ridge (Peng *et al*. 2011). Combining the advantages of STFT and WT, Stockwell *et al*. (1996) proposed ST. However, due to the fixed window function, its practical application is still limited.

Chirplet transform (CT) is a parametrized time-frequency transform, which can be regarded as a generalization of STFT (Mann and Haykin 1995). It is often used to analyze linear frequency modulation signals (Mann and Haykin 1992, Mihovilović and Bracewell 1992). CT can adjust each atom in the time-frequency plane by choosing appropriate frequency modulation parameters, thus, obtaining higher energy concentration (Jin *et al*. 2017). Angrisani and D'Arco (2002) presented a measurement method based on a modified version of the chirplet transform for IF estimation. However, when the IF of the signal is nonlinear, the traditional CT is not applicable. To solve this problem, Yang *et al*. (2011, 2014) improved the traditional CT and proposed the spline-kernelled chirplet transform (SCT). SCT can obtain the parameters of the spline kernel by spline approximation, so it has a high energy concentration when identifying nonlinear signals. In order to reduce the workload caused by kernel function fitting, Yu and Zhou (2016) creatively introduced rotation factors and proposed the generalized linear chirplet transform, which effectively improved the computational efficiency. Guan *et al*. (2018) put forward velocity synchronous linear chirplet transform in combination with a kurtosis-guided method. Hartono *et al*. (2019) conducted gear fault diagnosis using the general linear chirplet transform with vibration and acoustic measurements.

Furthermore, Abratkiewicz (2020) put forward double-adaptive chirplet transform for radar signature extraction.

*Corresponding author, Ph.D., Associate Professor,
E-mail: yuanpingping@just.edu.cn
[a] Associate Professor, E-mail: dyxue2008@163.com
[b] Graduate Student, E-mail: 3435519317@qq.com
[c] Professor, E-mail: renwx@szu.edu.cn

ISSN: 1738-1584 (Print), 1738-1991 (Online)

Guan and Feng (2021) proposed an adaptive linear chirplet transform for analyzing signals with crossing frequency trajectories. By introducing a kernel function that can be modulated with time and frequency, Li *et al*. (2020) originally proposed the scale-based chirplet transform. Zhu *et al*. (2019b) proposed synchroextracting chirplet transform for accurate IF estimate and perfect signal reconstruction. Senthil Pandi *et al*. (2022) introduced an optimal self-adaptive deep neural network and spine-kernelled chirplet transform for image registration.

To further improve energy aggregation, in this paper, the window function of SCT is improved, and a method called MSCT is proposed by using the principle of energy concentration (concentration measure, CM) (Yuan *et al*. 2022) to select the parameters of the window function. The IF extraction is performed on single component signal, multi-component signal, single degree of freedom Duffing system, and two-layer shear frame structure, respectively. At the same time, in order to validate the effectiveness of this method for practical structures, in the experimental aspect, the cable structure with time-varying stiffness is selected for experiment. The IF extracted by MSCT is compared with the IF extracted by STFT, ST, CT, and theoretical frequency to verify the effectiveness and superiority of the proposed method. At last, this paper ends up with some conclusions and lists some recommendations for future work.

2. Theoretical basis

2.1 CT and SCT

CT is an effective TFA method for processing linear frequency modulated signals. It introduces the concept of frequency rotation operator and frequency shift operator, and describes the kernel function by linear frequency modulated parameters to process linear frequency modulated signals. For a frequency-modulated time-varying signal $s(t)$, its CT is

$$\begin{aligned} &CT_s(t_0, f, \alpha; \sigma) \\ &= \int_{-\infty}^{+\infty} z(t)\ \psi(t, t_0, \alpha, \sigma)\, exp(-j2\pi f t)dt \end{aligned} \tag{1}$$

where, $z(t)$ is the analytical signal of $s(t)$, which can be expressed as $z(t) = s(t) + \mathrm{jH}[s(t)]$. Where $H[\cdot]$ is the Hilbert transform. $\psi(t, t_0, \alpha, \sigma)$ denotes a complex window function as follows

$$\psi(t, t_0, \alpha, \sigma) = w_\sigma(t - t_0)\, exp(-j\alpha(t - t_0)^2/2) \tag{2}$$

where, w_σ stands for a nonnegative symmetric normalized Gaussian window function which can be defined as

$$w_\sigma(t) = \frac{1}{\sqrt{2\pi}\sigma} exp\left(-\frac{1}{2}\left(\frac{t}{\sigma}\right)^2\right) \tag{3}$$

According to the analysis of the definition, CT is STFT of the product of analytic signal and window function, which is essentially Fourier transform of signal with frequency modulated window. Therefore, the definition of CT can also be expressed as

$$\begin{aligned} &CT_s(t_0, f, \alpha; \sigma) \\ &\quad = A(t_0, \alpha) \int_{-\infty}^{+\infty} \bar{z}(t)\, w_\sigma(t - t_0)\, exp(-j2\pi f t)dt \\ &\bar{z}(t) = z(t)\Phi^R(t, \alpha)\Phi^S(t, t_0, \alpha) \\ &\Phi^R(t, \alpha) = exp(-j\alpha t^2/2) \\ &\Phi^S(t, t_0, \alpha) = exp(-j\alpha t_0 t) \\ &A(t_0, \alpha) = exp(-j\alpha t_0^2/2) \end{aligned} \tag{4}$$

in which, $\Phi^R(t, \alpha)$ represents the frequency rotation operator, $\Phi^S(t, t_0, \alpha)$ represents the frequency shift operator. The rotation operator is to rotate analytic signal $z(t)$ in the time-frequency plane by θ degree, and $\tan(\theta) = -\alpha$; the shift operator is to translate frequency component at t_0 upwards by αt_0; $A(t_0, \alpha)$ is a complex number and $|A(t_0, \alpha)| = 1$.

When the IF of the signal is a nonlinear time-varying function, the traditional CT is no longer applicable throughout the entire time domain, and even cannot estimate the IF trajectory. To solve the problem, this paper introduces spline interpolation function as kernel function of CT to process nonlinear frequency modulated signal, namely SCT

$$\begin{aligned} &SCT_s(t_0, f, Q; \sigma) \\ &\quad = A(t_0, \alpha) \int_{-\infty}^{+\infty} \bar{z}(t)\, w_\sigma(t - t_0)\, exp(-j2\pi f t)dt \\ &t_0 \in (t_i, t_{i+1}) \\ &\bar{z}(t) = z(t)\Phi^R(t, Q)\Phi^S(t, t_0, Q) \\ &\Phi^R(t, Q) = exp\left(-j\sum_{k=1}^{n} \frac{q_k^i}{k}(t - t_i)^k + \gamma_i\right) \\ &\Phi^S(t, t_0, Q) = exp\left(j\sum_{k=1}^{n} q_k^i\,(t_0 - t_i)^{k-1} t\right) \end{aligned} \tag{5}$$

where, $\Phi^R(t, Q)$ and $\Phi^S(t, t_0, Q)$ are frequency-rotate operator and frequency-shift operator, respectively. $Q(i, k) = q_k^i$ represents the polynomial coefficient matrix of spline interpolated kernel function. The coefficient γ_i meets the following condition

$$\gamma_i - \gamma_{i+1} = \sum_{k=1}^{n} \frac{q_k^{i+1}}{k}(t_i - t_{i+1})^k \tag{6}$$

with $\gamma_1 = 0$.

2.2 MSCT

To further enhance the accuracy of IF extraction from structural non-stationary responses, many scholars have improved the window function accordingly. In this paper, we introduce a new Gaussian window with the following standard deviation

$$\sigma(f) = \frac{1}{\lambda_1(f + \lambda_2)^{\lambda_3}} \tag{7}$$

in which, the adjustment factors are introduced to further

speed up or slow down the change of window function with signal frequency, so the modified Gaussian window function can be obtained

$$w(t,f)=\frac{\lambda_1(f+\lambda_2)^{\lambda_3}}{\sqrt{2\pi}}\exp\left(\frac{-\lambda_1^2(f+\lambda_2)^{2\lambda_3}t^2}{2}\right) \quad (8)$$

Compared with the Gaussian window function, the modified Gaussian window function only replaces $|f|$ with $\lambda_1(f+\lambda_2)^{\lambda_3}$, so it also satisfies the normalized condition

$$\int_{-\infty}^{+\infty} w(t,f)dt=1 \quad (9)$$

It can be known that, when $\lambda_1=1$, $\lambda_2=0$ and $\lambda_3=1$, the modified window function changes back to the original standard Gaussian window function.

In the TFA, the mold of time-frequency distribution has practical significance. Therefore, substituting the modified window function into SCT, MSCT can be simplified as

$$\begin{aligned}&MSCT_s(t_0,f,Q;\sigma)\\&\quad=\int_{-\infty}^{+\infty}\bar{z}(t)\,w(t-t_0,\omega)\,exp(-j2\pi ft)dt\\&t_0\in(t_i,t_{i+1})\\&\bar{z}(t)=z(t)\Phi^R(t,Q)\Phi^S(t,t_0,Q)\\&\Phi^R(t,Q)=exp\left(-j\sum_{k=1}^{n}\frac{q_k^i}{k}(t-t_i)^k+\gamma_i\right)\\&\Phi^s(t,t_0,Q)=exp\left(j\sum_{k=1}^{n}q_k^i\,(t_0-t_i)^{k-1}t\right)\end{aligned} \quad (10)$$

Based on the principle of energy CM expressed in the following equation, the parameters of the window function can be determined by solving the optimization problem.

$$\begin{aligned}&CM(\lambda_1,\lambda_2,\lambda_3)=\frac{1}{\int_{-\infty}^{+\infty}\int_{-\infty}^{+\infty}\left|\overline{MSCT_s^{\lambda_1,\lambda_2,\lambda_3}(t,f)}\right|dtdf}\\&\overline{MSCT_s^{\lambda_1,\lambda_2,\lambda_3}(t,f)}\\&\quad=\frac{MSCT_s^{\lambda_1,\lambda_2,\lambda_3}(t,f)}{\sqrt{\int_{-\infty}^{+\infty}\int_{-\infty}^{+\infty}\left|MSCT_s^{\lambda_1,\lambda_2,\lambda_3}(t,f)\right|^2dtdf}}\end{aligned} \quad (11)$$

$$\arg\max_{\lambda_1,\lambda_2,\lambda_3}\frac{1}{\int_{-\infty}^{+\infty}\int_{-\infty}^{+\infty}\left|\overline{MSCT_s^{\lambda_1,\lambda_2,\lambda_3}(t,f)}\right|dtdf} \quad (12)$$

The constraint conditions of the optimization problem are related to the width range of the analyzed window. The window should not be too narrow to change the time resolution, but it should also not be too wide to affect the frequency resolution, that is

$$KT_s\le\frac{1}{\lambda_1(f+\lambda_2)^{\lambda_3}}\le LT \quad (13)$$

where, T_s is the sampling period, $f\in[f_{\min},\ f_{\max}]$, $f_{\min}$ is generally set to 1 Hz. To satisfy the Nyquist sampling theorem, the value of $f_{\max}$ takes half of the sampling frequency.

By referring to related literatures, we can let $\lambda_1\in(0,3]$, $\lambda_2\in[0,3]$, $\lambda_3\in[0,1]$, $K=10$ and $L=1000$. The parameters can also be adjusted slightly according to the actual situation. So, the final optimization problem is as follows

$$\begin{cases}\arg\max\limits_{\lambda_1,\lambda_2,\lambda_3}\dfrac{1}{\sum_1^N\sum_{f_{\min}}^{f_{\max}}\left|\overline{MSCT_s^{\lambda_1,\lambda_2,\lambda_3}(t,f)}\right|}\\S_c:\ KT_s\lambda_1(f_{\max}+\lambda_2)^{\lambda_3}-1\le0\\\quad 1-\lambda_1(f_{\min}+\lambda_2)^{\lambda_3}LT_s\le0\\\quad 0<\lambda_1\le3\\\quad 0\le\lambda_2\le3\\\quad 0\le\lambda_3\le1\end{cases} \quad (14)$$

To summarize, the proposed MSCT algorithm can be expressed as follows.

Algorithm: MSCT

Step 1: Substitute the modified Gaussian window function into the CT and conduct parameters optimization of the modified CT

Step 2: Calculate the modified CT coefficient with the optimized parameters and conduct spline interpolation of kernel function

Step 3: Substitute the obtained kernel function into the SCT and conduct parameters optimization of the SCT

Step 4: Calculate the MSCT coefficient with the optimized parameters

Step 5: Extract IF according to the MSCT coefficient

3. Analytical signal analysis

3.1 Single-component signal

The ability of MSCT to process single-component signals is explored by establishing signal S_1 for numerical simulation. The signal is defined as follows

$$S_1=sin\left(2\pi\left(5t+\frac{5}{4}t^2+\frac{1}{6}t^3-\frac{1}{160}t^4\right)\right) \quad (15)$$

The sampling frequency of this signal is 300 Hz and the sampling time is 10 s. Fig. 1 is the time domain diagram of

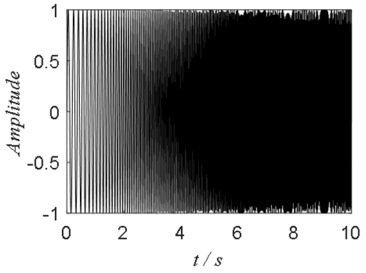

Fig. 1 The simulated single-component signal

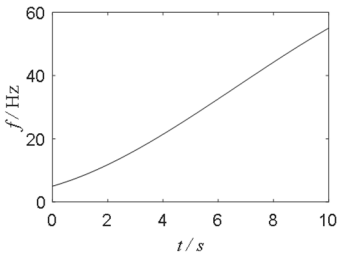

Fig. 2 The theoretical frequency of single-component signal

signal S_1, and Fig. 2 is its theoretical frequency. The signal is processed by STFT, ST, CT and MSCT, respectively, and the time-frequency results are shown in Fig. 3. In this figure, time-frequency representations of the four methods and their corresponding local enlarged images are displayed in the subgraphs of Figs. 3(a)-(c). It can be observed that the energy diffusion of ST is serious, especially after 2 s, while the energy of STFT, CT and MSCT are all concentrated within a certain bandwidth. By comparing Fig. 3(a), Fig. 3(e) and Fig. 3(g), we can know that MSCT has the narrowest energy bandwidth, which indicates that its energy is most concentrated.

The IFs of STFT, ST, CT and MSCT time-frequency representations are extracted and compared with the theoretical frequency. Shown in Fig. 4, it can be clearly known that all the four methods can effectively identify the IF, and the extracted results are all close to the theoretical frequency. In order to evaluate the accuracy of IF recognition, the accuracy index (AI) defined by relative standard deviation between extracted IF and theoretical IF is introduced. The smaller the AI value, the higher the identification accuracy. The computing formula of AI is

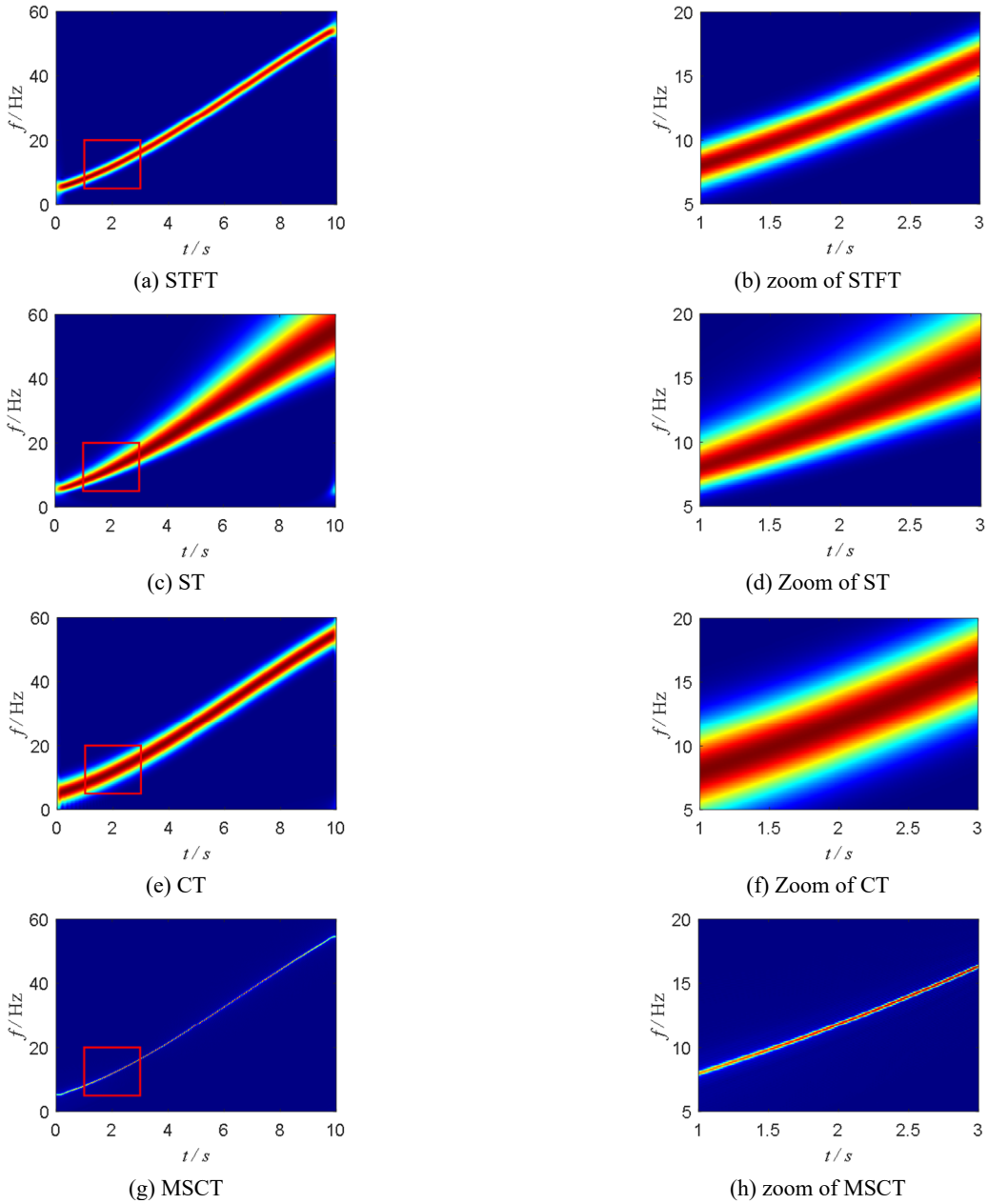

Fig. 3 The time-frequency results of single-component signal

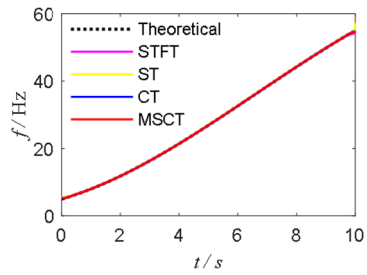

Fig. 4 Comparison of theoretical IF and identified IF of single-component signal

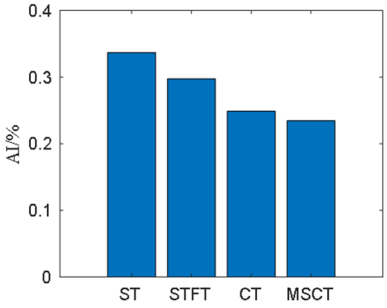

Fig. 5 The AI value of IF recognition of single-component signal

expressed as

$$\mathrm{AI}=\frac{\sqrt{\int_0^T[f_e(t)-f_t(t)]^2dt}}{\sqrt{\int_0^T[f_t(t)]^2dt}} \tag{16}$$

in which, $f_e(t)$ is extracted IF and $f_t(t)$ represents theoretical IF. The smaller the AI value, the closer the extracted IF is to the theoretical IF.

The AI values of STFT, ST, CT and MSCT results are calculated and shown in Fig. 5. Obviously, among these four methods, MSCT has the smallest AI value, which indicates that MSCT has the highest recognition accuracy. In summary, the TFA of MSCT is effective and feasible.

To show the computation complexity, Table 1 lists the computation time of the single-component signal processed by the STFT, ST, CT and MSCT. These calculations are carried out on a 64-bit Windows computer equipped with Intel Core i5 processor, running MATLAB R2021b. The computation time of the MSCT appears to be approximately eight times that of the CT. However, it should be noted that most of the time is spent on the iterative calculations for optimizing parameters. Overall, the computation time of the MSCT is still not too long, and the computational efficiency is still within an acceptable range.

To further verify the noise resistance and energy concentration of MSCT, Gaussian white noise is added to the original signal during the analysis process, and signal-to-noise ratio (SNR) (Yuan *et al*. 2021) is selected as noise index. Then, the noisy signal can be analyzed by STFT, ST, CT, and MSCT, and the Rényi entropy (Chen *et al*. 2019) of the TFA results can be calculated. The calculation methods of SNR and Rényi entropy are as follows

Table 1 Computation time of different TFA methods of single-component signal

Method	STFT	ST	CT	MSCT
Computation time (s)	1.062	0.681	2.808	21.126

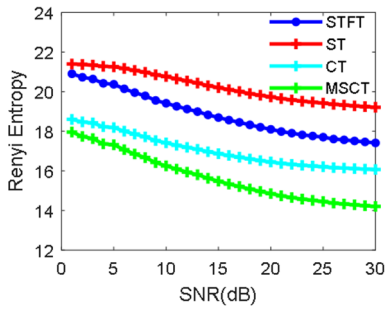

Fig. 6 Rényi entropies of different TFA methods of single-component signal

$$SNR=10\log\frac{||f_0||^2}{||f-f_0||^2} \tag{17}$$

$$R_c^{\alpha}=\frac{1}{1-\alpha}\log_2\int_{-\infty}^{+\infty}\int_{-\infty}^{+\infty}C_x(t,f)\,dtdf \quad (\alpha>0 \ \text{且} \ \alpha\neq 0) \tag{18}$$

where f_0 is the original signal and f is the reconstructed signal. R_c^{α} is the calculated Rényi entropy, is $C_x(t,f)$ the two-dimensional time-frequency distribution data in the TFA results, and α is the entropy index. For time-frequency distribution, entropy index can be set as $\alpha=3$ (Guan and Feng 2021). As the SNR increases, the Rényi entropy decreases. The smaller the Rényi entropy, the stronger the anti-noise ability.

The Gaussian white noises with SNR = 1~30 dB are added to the signal S_1, and TFA of the noisy signals is performed again using the four methods of STFT, ST, CT and MSCT. At the same time, the Rényi entropy of each TFA method under different SNR are obtained and shown in Fig. 6. For better comparison, Table 2 lists the Rényi entropies calculated by different methods when SNR= dB, SNR = 15 dB and SNR = 25 dB. It can be known that the corresponding Rényi entropy of each method decreases when the SNR increases. However, under the same SNR, the Rényi entropy of MSCT TFA results is smaller than that of the other three processing methods under 1~30 dB Gaussian white noise. This shows that the noise resistance and energy concentration of MSCT is better than that of the

Table 2 Rényi entropies of different TFA methods of single-component signal

Method	STFT	ST	CT	MSCT
Rényi entropy (5 dB)	20.373	21.260	18.185	17.317
Rényi entropy (15 dB)	18.692	20.206	16.866	15.476
Rényi entropy (25 dB)	17.702	19.424	16.209	14.450

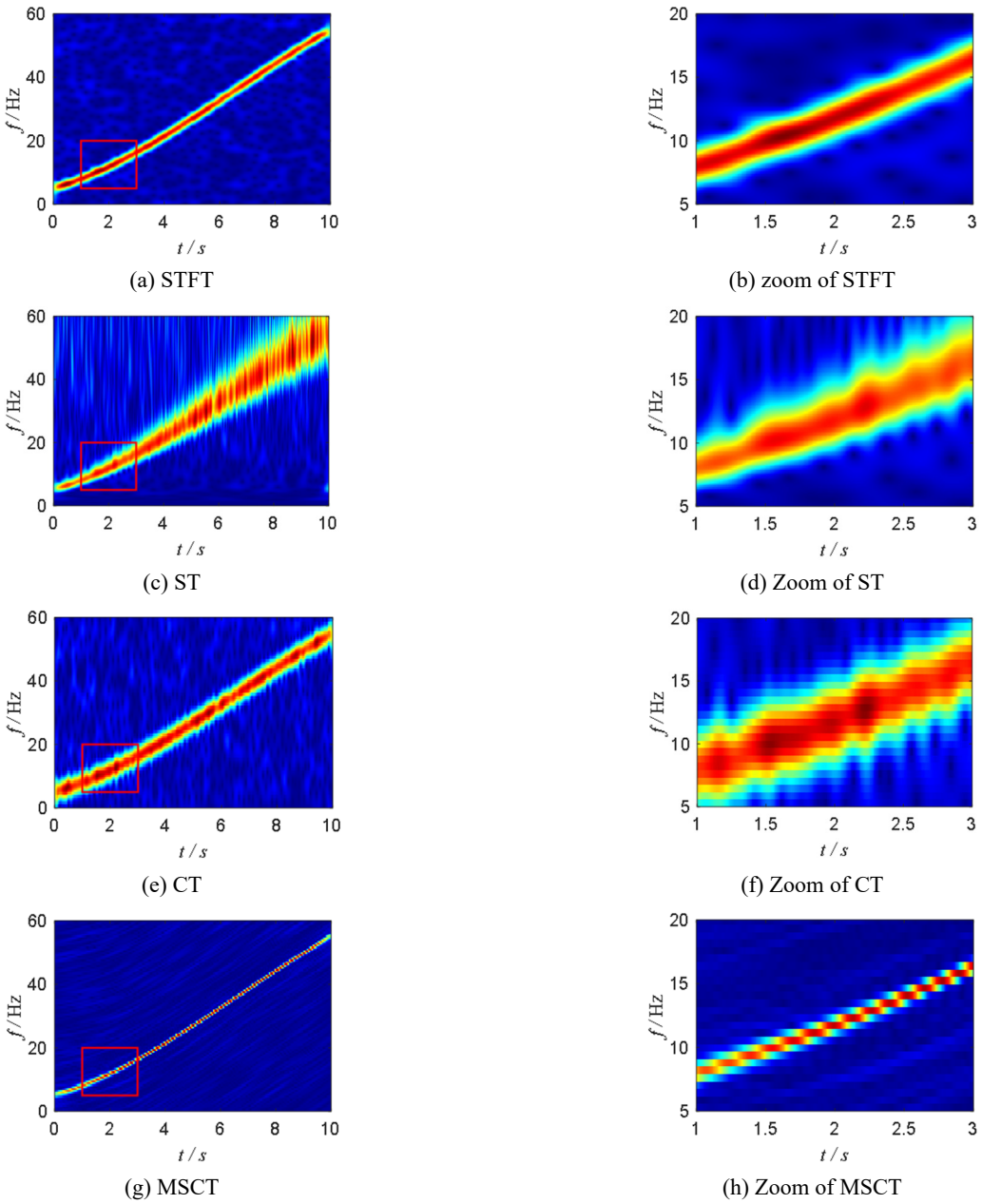

(a) STFT (b) zoom of STFT

(c) ST (d) Zoom of ST

(e) CT (f) Zoom of CT

(g) MSCT (h) Zoom of MSCT

Fig. 7 The time-frequency results of single-component signal when SNR = 10 dB

other three methods.

Fig. 7 shows the results (SNR = 10 dB) after processing by different TFA methods. Obviously, MSCT has the best energy concentration, while the energy concentration of STFT, ST or CT is not as good as that of MSCT. Therefore, when processing single-component signals, MSCT has better recognition performance, better anti-noise ability and better energy concentration. It can be used as an effective and reliable TFA method.

3.2 Multi-component signal

In order to investigate the ability of MSCT to process multi-component signals, in this paper, a two-component signal is selected and defined as follows

$$S_2 = \begin{cases} x_1(t) = sin(\,2\pi(150t + 20t^3)) \\ x_2(t) = sin(\,2\pi(300t + 100t^4)) \end{cases} \tag{19}$$

The sampling frequency of this signal is 2000 Hz and the sampling time is 1 s. Fig. 8 is the time domain diagram of signal S_2, and Fig. 9 is its theoretical frequency.

The signal is processed by the same methods, and the time-frequency representations are shown in Fig. 10. Among them, Figs. 10(a)-(d) are the time-frequency results of STFT, ST, CT and MSCT. It is obvious that the energy concentration of ST result is poor, and the energy diffusion is more serious after 0.4 s. The energy of STFT, CT and MSCT are all concentrated within a certain bandwidth for each component signal, which indicates that they can effectively identify IFs of S_2. The IFs of STFT, ST, CT and MSCT representations are extracted and compared with

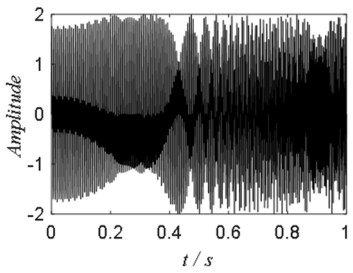

Fig. 8 The simulated multi-component signal

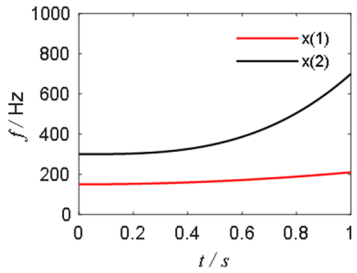

Fig. 9 The theoretical frequency of multi-component signal

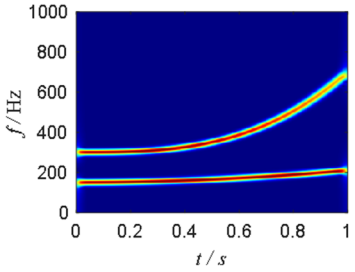

(a) STFT

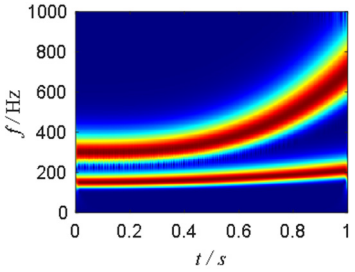

(b) ST

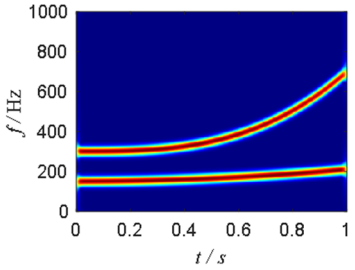

(c) CT

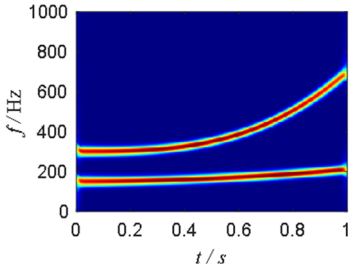

(d) MSCT

Fig. 10 The time-frequency results of multi-component signal

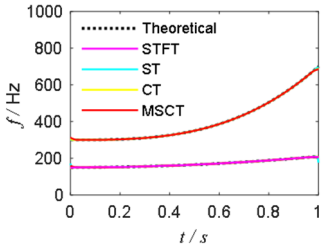

Fig. 11 Comparison of theoretical IF and identified IF of multi-component signal

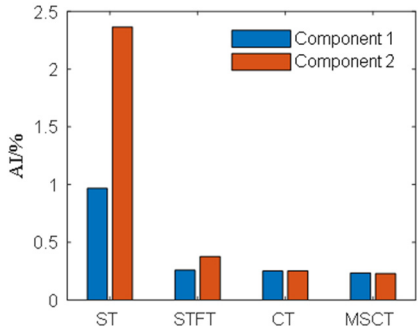

Fig. 12 The AI value of IF recognition of multi-component signal

the theoretical frequency. Shown in Fig. 11, it can be clearly known that all the four methods can effectively identify the IF, and the extracted results are all close to the theoretical frequency. In order to evaluate the accuracy of IF recognition, the AI values of STFT, ST, CT and MSCT results are calculated and shown in Fig. 12. It can be clearly seen that for the component signal x_1 and x_2, the recognition accuracy AI value of MSCT is smaller, which indicates that the IF of MSCT recognition is closer to theoretical value. In summary, the TFA of MSCT is effective and feasible for signal processing.

Again, different levels of Gaussian white noises (SNR = 1~30 dB) are added to the signal S_2, and STFT, ST, CT and MSCT are used to analyze the signal in time-frequency domain. At the same time, Rényi entropies of each method under different noises are obtained and shown in Fig. 13. Table 3 lists the Rényi entropies when SNR = 5 dB, SNR = 15 dB and SNR = 25 dB. It can be seen from Fig. 13 and Table 3 that the Rényi entropy of MSCT is smaller than the other three methods under the same SNR, which indicates that the time-frequency concentration and anti-noise ability of MSCT are better.

Fig. 14 gives the TFA results of different methods for

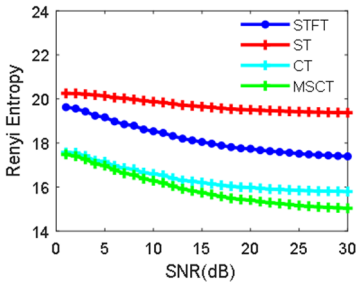

Fig. 13 Rényi entropies of different TFA methods of multi-component signal

signal S_2 when SNR = 10 dB. Through the comparison of these four figures, we can know that the time-frequency concentration of STFT and MSCT is higher, while the diffusion of ST and CT is more serious when SNR = 10 dB. Therefore, MSCT has better anti-noise ability and better energy concentration when processing multi-component signals. It can be used as an effective and reliable TFA method.

Table 3 Rényi entropies of different TFA methods of multi-component signal

Method	STFT	ST	CT	MSCT
Rényi entropy (5 dB)	19.167	20.135	17.153	16.973
Rényi entropy (15 dB)	18.049	19.649	16.203	15.747
Rényi entropy (25 dB)	17.513	19.418	15.847	15.157

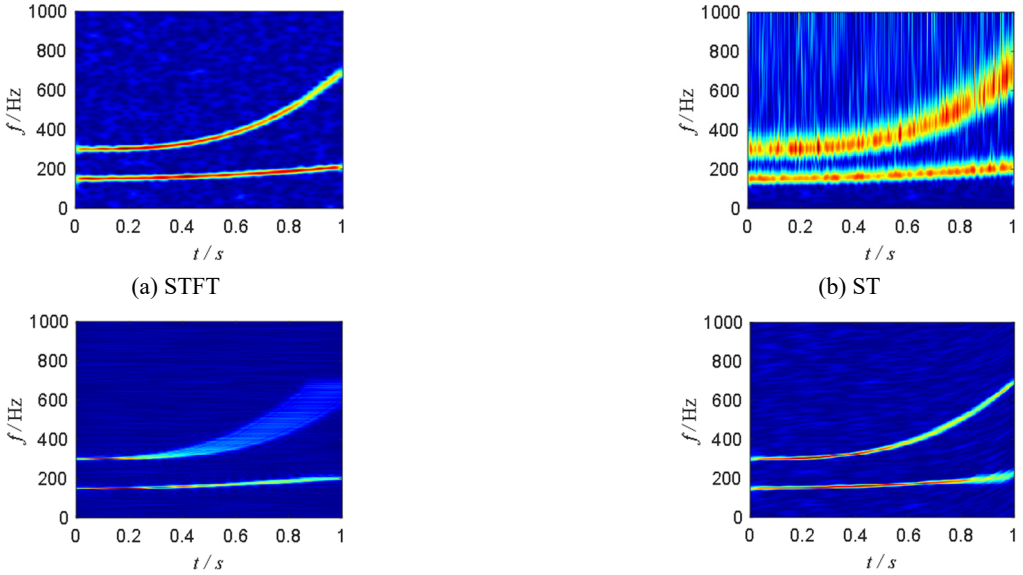

(a) STFT (b) ST

(c) CT (d) MSCT

Fig. 14 The time-frequency results of multi-component signal when SNR = 10 dB

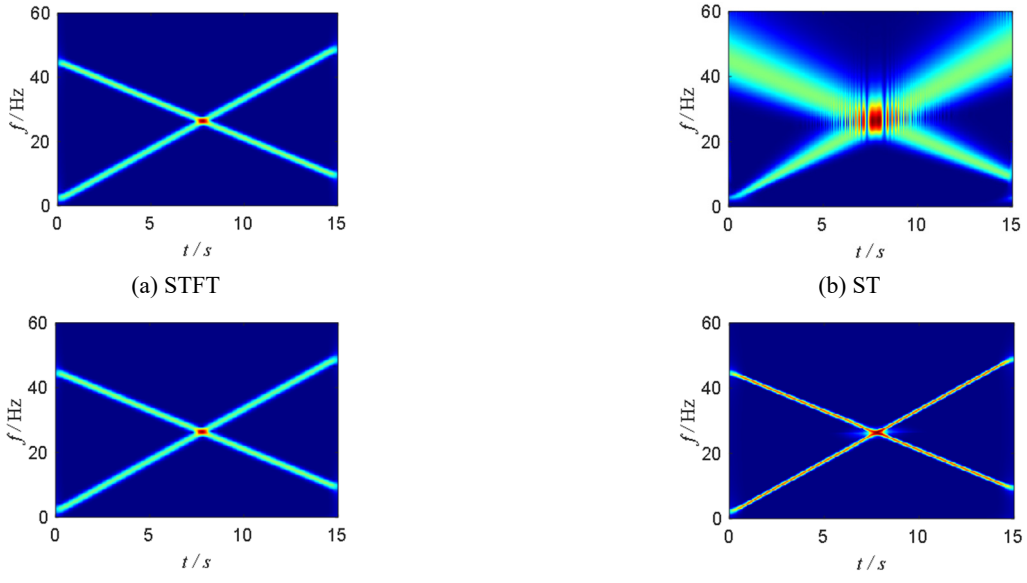

(a) STFT (b) ST

(c) CT (d) MSCT

Fig. 15 The time-frequency results of multi-component signal with crossed IFs

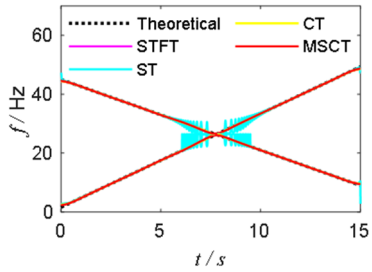

Fig. 16 Comparison of theoretical IF and identified IF of multi-component signal with crossed IFs

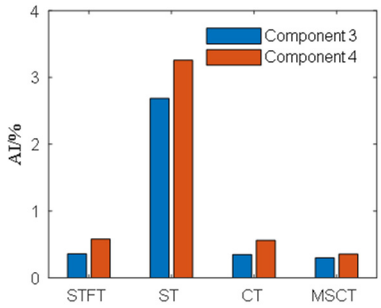

Fig. 17 The AI value of IF recognition of multi-component signal with crossed IFs

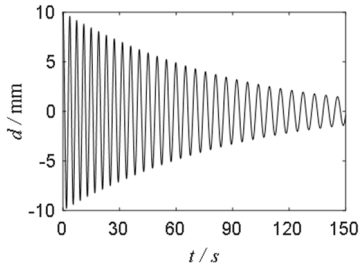

Fig. 18 Structural displacement response of Duffing system

The numerical multiple components above have the well-separated IFs. However, it is necessary to consider the signal with crossed IFs, which are often encountered in practice. Given the numerical signal as

$$S_3 = \begin{cases} x_3(t) = cos\left(2\pi(0.35 + 45t - 1.2t^2)\right) \\ x_4(t) = cos(10t + 10t^2) \end{cases} \quad (20)$$

To demonstrate the performance of the MISC more clearly, we list the time-frequency representations, extracted IFs and AI values as shown in Figs. 15-17. It can be seen from these figures that, the ST gets lower concentration measure than STFT and CT, and the proposed scheme obtains the best concentration and resolution, which indicates the MSCT can extract IFs of signal with crossing frequency trajectory effectively.

4. Structural simulation

4.1 Nonlinear structure under free vibration

To further explore the ability of MSCT to analyze and process single-degree-of-freedom structural non-stationary free vibration signal, the classical Duffing system is introduced to simulate a nonlinear structural system, and the free vibration equation of the nonlinear system is

$$\ddot{y} + 0.03\dot{y} + y + 0.01y^3 = 0 \quad (21)$$

The initial conditions are $y_0 = 10$ and $\dot{y}_0 = 0$. The Runge-Kutta method is used to obtain the structural displacement response. The duration and interval are $t = 100\,s$ and $\Delta t = 0.1\,s$. The displacement response of Duffing system is shown in Fig. 18.

Fig. 19 gives the time-frequency results of displacement response of Duffing system by using four methods. From

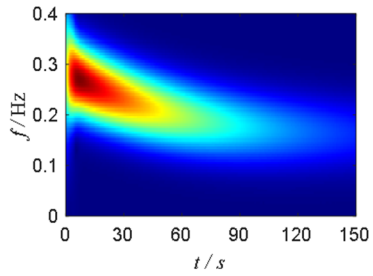

(a) STFT

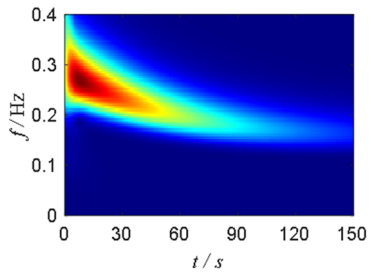

(b) ST

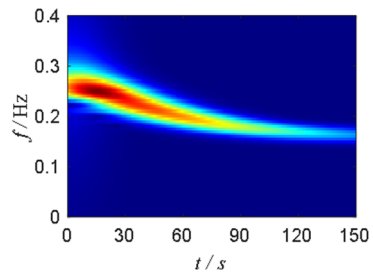

(c) CT

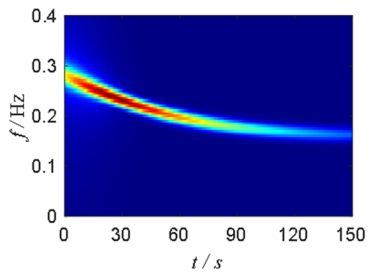

(d) MSCT

Fig. 19 The time-frequency results of displacement response of Duffing system

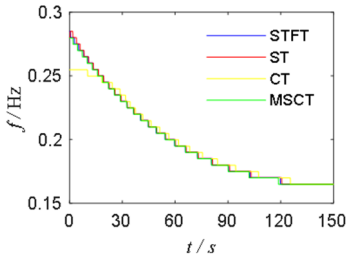

Fig. 20 The identified IF of displacement response of Duffing system

this figure, it is evident that MSCT has a higher time-frequency concentration, while STFT, ST and CT exhibit more severe energy diffusion during the initial stage of vibration. The IF is extracted by the extreme value method and shown in Fig. 20. It can be seen from this figure that there is a certain difference between CT and the other three methods at the initial point, which indicates that CT cannot effectively identify the initial frequency. In summary, MSCT is more accurate for the IF identification of nonlinear single-degree-of-freedom structure.

4.2 Two-story frame structure under forced vibration

In order to further explore the TFA ability of MSCT for stiffness-varying structures, this paper selects a two-story frame structure for numerical simulation. The two-story frame structure is shown in Fig. 21, and the physical parameters of this structure are shown in Table 4.

The dynamic equation of the frame structure is

$$\begin{cases} m_1\ddot{y}_1 + (c_1 + c_2)\dot{y}_1 - c_2\dot{y}_2 + (k_1 + k_2)y_1 \\ \qquad - k_2y_2 = f_1 \\ m_2\ddot{y}_2 - c_2\dot{y}_1 + c_2\dot{y}_2 - k_2y_1 + k_2y_2 = f_2 \end{cases} \tag{21}$$

where, the time-varying stiffness k_1 and k_2 meet the following conditions

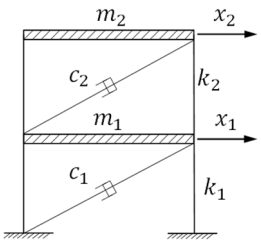

Fig. 21 Two-story frame structure

Table 4 Parameters of two-story frame structure

Layer	Quality m/kg	Damping coefficient c/(N·s·m^{-1})	Initial stiffnes k/(N·m^{-1})
First	2.76×10^5	5.60×10^5	2.52×10^8
Second	1.62×10^5	1.62×10^5	1.30×10^8

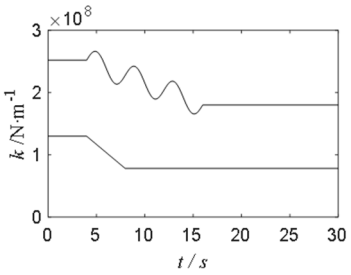

(a) Stiffness

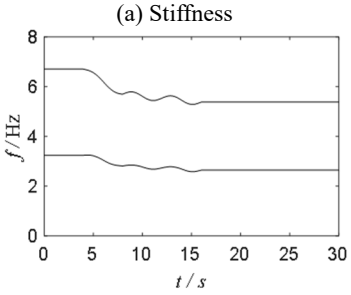

(b) IF

Fig. 22 The time-varying stiffness and theoretical IF of frame structure

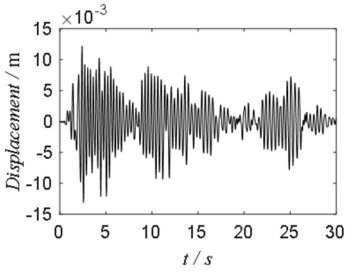

Fig. 23 Displacement response of the first layer under EL-Centro earthquake

$$k_1 = \begin{cases} 2.52 \times 10^8, & 0 \le t < 4 \\ \{2.4 - 0.06 \times (t-6) \\ -0.2 \times sin[\frac{\pi}{2}(t-6)]\} \times 10^8, & 4 \le t < 16 \\ 1.80 \times 10^8, & 16 \le t < 25 \end{cases} \tag{22}$$

$$k_2 = \begin{cases} 1.30 \times 10^8, & 0 \le t < 4 \\ [1.30 - 0.13 \times (t-4)] \times 10^8, & \\ & 4 \le t < 8 \\ 0.78 \times 10^8, & 8 \le t < 25 \end{cases}$$

The curve of time-varying stiffness is shown in Fig. 22(a). By calculating matrix eigenvalues, the theoretical IF trajectory of the frame structure can be obtained and shown in Fig. 22(b).

The dynamic response of this two-story frame structure under EL-Centro earthquake is obtained by time-history analysis with Runge-Kutta method. The sampling frequency is 50 Hz and the sampling time is 30 s. Fig. 23 is the displacement response of the first layer.

TFA of displacement response signal of the first layer under EL-Centro earthquake excitation is performed by STFT, ST, CT and MSCT, and the TFA results are shown in

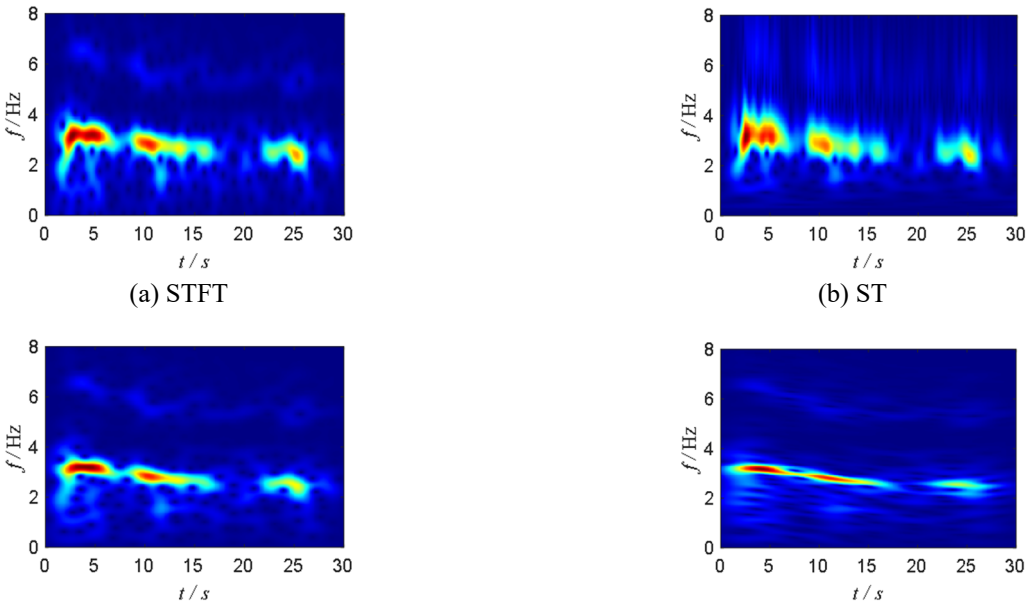

(a) STFT (b) ST

(c) CT (d) MSCT

Fig. 24 The time-frequency results under EL-Centro earthquake

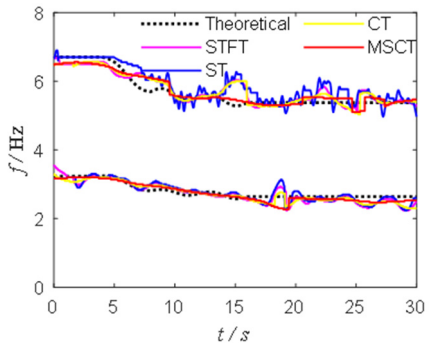

Fig. 25 The identified IF under EL-Centro earthquake

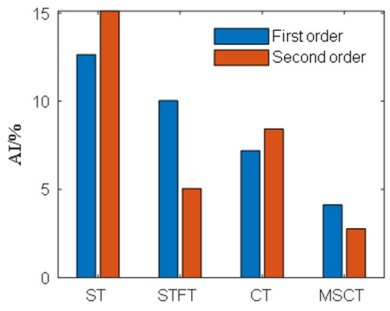

Fig. 26 The AI value of IF recognition under EL-Centro earthquake

Fig. 24. By comparing Figs. 24(a)-(d), we can know that MSCT has the narrowest energy bandwidth, which indicates that its energy is most concentrated. The IF is extracted by the extreme value method and compared with the theoretical frequency. Shown in Fig. 25, we can know that MSCT results are closer to the theoretical values and smoother. In summary, MSCT has a good TFA effect and high accuracy for stiffness-varying structures.

To evaluate the accuracy of IF recognition, the AI values of STFT, ST, CT and MSCT results are calculated and shown in Fig. 26. It can be clearly seen that the recognition accuracy AI value of MSCT is smaller, which indicates that the IF of MSCT recognition is closer to theoretical value. Therefore, the TFA of MSCT is effective and feasible for time-varying structures.

5. Experimental verification

5.1 Nonlinear supported beam structure

In order to explore the recognition accuracy of MSCT in practical engineering, a cable structure with time-varying stiffness is selected for experimental verification. Fig. 27 shows test design and cable test device. One end of the cable is fixed on the reaction frame, and the other end is pulled by the MTS loader. The cable is made of a 4.55 m long steel strand of 7Φ5 with elastic modulus $E = 1.95 \times 10^5$ Mpa and cross-sectional area of $A = 1.374 \times 10^{-4}$ m^2 .In order to ensure that the stiffness changes with time, the tension on the cable is stably changed with time. The acceleration sensor is installed in the middle of the cable, and the sampling frequency is set 600 Hz. The experimental data are obtained by hammering the cable.

The linear varying tension force is applied on the cable. The initial tension is 20 kN, and the increasing speed is 1.67 kN/s. The impact hammer is used to hammer the cable. Force and acceleration signals are measured and the collection time is 6 s. The linear changing of the actual tension and the acceleration response are shown in Figs. 28(a)-(b), respectively.

TFA of the acceleration response is conducted by STFT, ST, CT and MSCT. Fig. 29 is the time-frequency results of these four methods. It can be seen from this figure that ST

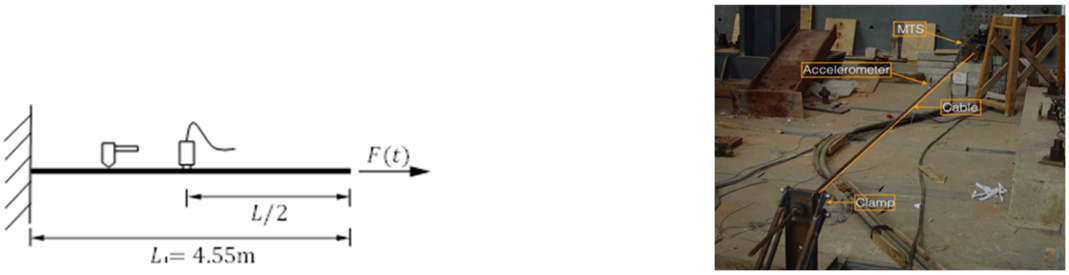

(a) Test design (b) Test device

Fig. 27 The cable test design and device

(a) Linear changing tension (b) Acceleration response

Fig. 28 Linear changing tension and acceleration response

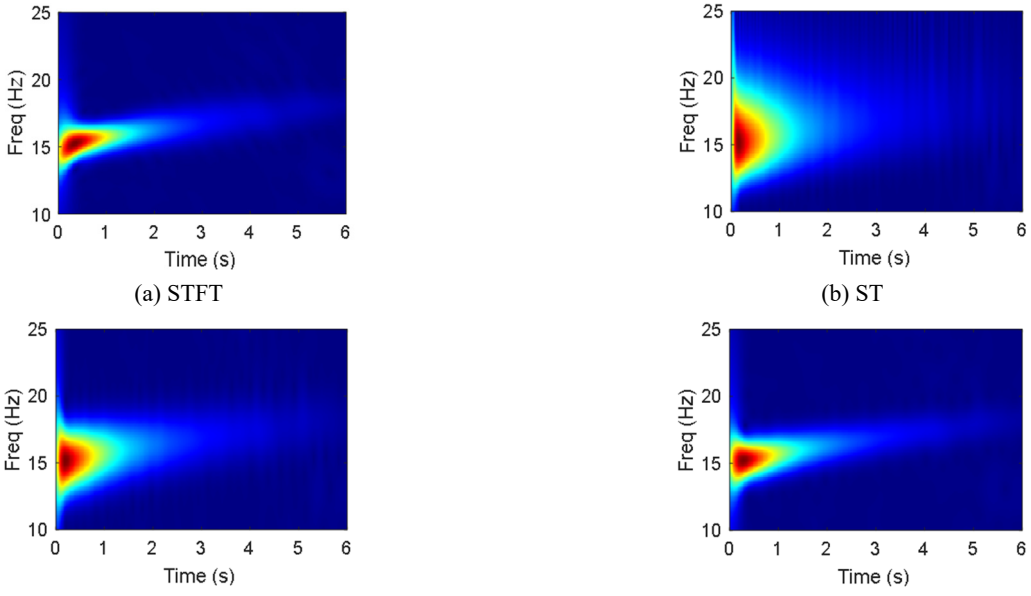

(a) STFT (b) ST

(c) CT (d) MSCT

Fig. 29 The time-frequency results under linear changing tension

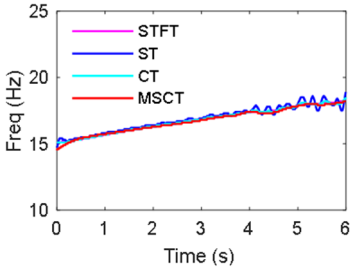

Fig. 30 The identified IF under linear changing tension

and CT have poor energy concentration at the endpoint, while the time-frequency results of STFT and MSCT are relatively clear. By extreme values extracting, Fig. 30 shows the IFs of STFT, ST, CT and MSCT. Obviously, the identification result of ST is blurred at the right endpoint, while the other three methods have better identification results. The experimental results show that the TFA of MSCT is clear and accurate, which can be used for structural IF extraction in practical engineering.

6. Conclusions

In this paper, the spline-kernelled chirplet transform is improved and a new TFA form named MSCT is proposed based on revised Gaussian window function and energy concentration principle. The TFA and IF extraction of single-component signal, multi-component signal, single-degree-of-freedom Duffing system, two-story shear frame structure and a cable structure with time-varying stiffness is carried out. Through numerical simulation and experimental verification, it is proved that the proposed MSCT method can effectively extract the IFs of nonlinear structure and time-varying structure.

Based on the results, it can be concluded that:

- The adjustment factors introduced in time window function can further speed up or slow down the change of window function with signal frequency, which can improve the time-frequency energy concentration and identify clearer time-frequency curve.
- Combined with the principle of energy concentration, the window function adjusting factors in MSCT can be calculated directly, which improves the computational efficiency and accuracy.
- Numerical simulation and experimental results show that the MCST method can effectively identify IF of nonlinear and time-varying structures with non-stationary response signals, and it has high accuracy and good stability.

Acknowledgments

Financial support to complete this study is provided in part by the National Natural Science Foundation of China (Grant No. 51979130) and Postdoctoral Research Funding Program of Jiangsu Province (Grant No. 2021K562C). The results and opinions expressed in this paper are those of the authors only and they don't necessarily represent those of the sponsors.

References

Abratkiewicz, K. (2020), "Double-adaptive chirplet transform for radar signature extraction", *IET Radar Sonar Nav*., **14**(10), 1463-1474. https://doi.org/10.1049/iet-rsn.2020.0084

Angrisani, L. and D'Arco, M. (2002), "A measurement method based on a modified version of the chirplet transform for instantaneous frequency estimation", *IEEE T. Instrum. Meas*., **51**(4), 704-711. https://doi.org/10.1109/TIM.2002.803295

Chen, P., Wang, K., Zuo, M.J. and Wei, D. (2019), "An ameliorated synchroextracting transform based on upgraded local instantaneous frequency approximation", *Measurement*, **148**, 106953. https://doi.org/10.1016/j.measurement.2019.106953

Djurović, I. and Stankovic, L.J. (2004), "An algorithm for the Wigner distribution based instantaneous frequency estimation in a high noise environment", *Signal Process*., **84**(3), 631-643. https://doi.org/10.1016/j.sigpro.2003.12.006

Guan, Y. and Feng, Z. (2021), "Adaptive linear chirplet transform for analyzing signals with crossing frequency trajectories", *IEEE Trans. Ind. Electron*., **69**(8), 8396-8410. https://doi.org/10.1109/TIE.2021.3097605

Guan, Y., Liang, M. and Necsulescu, D.S. (2018), "Velocity synchronous linear chirplet transform", *IEEE Trans. Ind. Electron*., **66**(8), 6270-6280. https://doi.org/10.1109/TIE.2018.2873520

Hartono, D., Halim, D. and Roberts, G.W. (2019), "Gear fault diagnosis using the general linear chirplet transform with vibration and acoustic measurements", *J. Low Freq. Noise V. A*., **38**(1), 36-52. https://doi.org/10.1177/1461348418811717

Jin, Y., Gao, D. and Ji, H.B. (2017), "Parameter estimation of LFM signals based on synchrosqueezing chirplet transform in complicated noise", *J. Electron. Inf. Techn*., **39**(08), 1906-1912. https://doi.org/10.11999/JEIT161222

Li, Z. and Crocker, M.J. (2006), "A study of joint time-frequency analysis-based modal analysis", *IEEE T. Instrum. Meas*., **55**(6), 2335-2342. https://doi.org/10.1109/TIM.2006.884137

Li, M., Wang, T., Chu, F., Han, Q. and Zhou, M. (2020), "Scaling-basis chirplet transform", *IEEE T. Ind. Electron*., **68**(9), 8777-8788. https://doi.org/10.1109/TIE.2020.3013537

Mann, S. and Haykin, S. (1992), "Adaptive chirplet transform: an adaptive generalization of the wavelet transform", *Opt. Eng*., **31**(6), 1243-1256. https://doi.org/10.1117/12.57676

Mann, S. and Haykin, S. (1995), "The chirplet transform: Physical considerations", *IEEE T. Signal Proces*., **43**(11), 2745-2761. https://doi.org/10.1109/78.482123

Mihovilović, D. and Bracewell, R.N. (1992), "Whistler analysis in the time-frequency plane using chirplets", *J. Geophys. Res.-Space*, **97**, 17199-17204. https://doi.org/10.1029/92JA01140

Pang, C.S., Liu, L. and Shan, T. (2014), "Time-frequency analysis method based on short time fractional Fourier transform", *Acta Electronica Sinica*, **42**(02), 347-352.

Peng, F., Yu, D. and Luo, J. (2011), "Sparse signal decomposition method based on multi-scale chirplet and its application to gear fault diagnosis", *Mech. Syst. Signal Pr*., **25**(2), 549-557. https://doi.org/10.1016/j.ymssp.2010.06.004

Senthil Pandi, S., Senthilselvi, A., Maragatharajan, M. and Manju, I. (2022), "An optimal self adaptive deep neural network and spine-kernelled chirplet transform for image registration", *Concurr. Comp.-Pract. E*., **34**(27), e7297. https://doi.org/10.1002/cpe.7297

Stockwell, R.G., Mansinha, L. and Lowe, R.P. (1996), "Localization of the complex spectrum: the S transform", *IEEE T. Signal Proces*., **44**(4), 998-1001. https://doi.org/10.1109/78.492555

Yan, H.S., Li, D. and Ding, L.G. (2015), "A new time-frequency analysis approach based on short time Fourier transform", *Acta Armamentarii*, **36**(S2), 258-261.

Yang, Y., Peng, Z.K., Meng, G. and Zhang, W.M. (2011), "Spline-kernelled chirplet transform for the analysis of signals with time-varying frequency and its application", *IEEE T. Ind. Electron*., **59**(3), 1612-1621. https://doi.org/10.1109/TIE.2011.2163376

Yang, Y., Peng, Z.K., Dong, X.J., Zhang, W.M. and Meng, G. (2014), "General parameterized time-frequency transform", *IEEE T. Signal Proces*., **62**(11), 2751-2764. https://doi.org/10.1109/TSP.2014.2314061

Yu, G. and Zhou, Y. (2016), "General linear chirplet transform", *Mech. Syst. Signal Pr*., **70**, 958-973. https://doi.org/10.1016/j.ymssp.2015.09.004

Yuan, P.P., Cheng, X.L., Wang H.H., Zhang, J., Shen, Z.X. and Ren, W.X. (2021), "Structural instantaneous frequency extraction based on improved multi-synchrosqueezing generalized S-transform", *Smart Struct. Syst*., *Int. J*., **28**(5), 675-687. https://doi.org/10.12989/sss.2021.28.5.675

Yuan, P.P., Zhang, J., Feng, J.Q., Wang, H.H., Ren, W.X. and Wang, C. (2022), "An improved time-frequency analysis method for structural instantaneous frequency identification

based on generalized S-transform and synchroextracting transform", *Eng*. *Struct*., **252**, 113657. https://doi.org/10.1016/j.engstruct.2021.113657

Zhang, L.X., Jia, Y.H., Xu, M.P., Hong, Z., Zhao, X., He, F., Wan, B.K. and Jiao, X.J. (2014), "Chirp stimuli visual evoked potential based brain-computer interface by chirplet transform algorithm", *Nanotechnol*. *Precis*. *Eng*., **12**(03), 157-161.

Zhu, X., Zhang, Z., Gao, J. and Li, W. (2019a), "Two robust approaches to multicomponent signal reconstruction from STFT ridges", *Mech*. *Syst*. *Signal Pr*., **115**, 720-735. https://doi.org/10.1016/j.ymssp.2018.06.047

Zhu, X., Zhang, Z., Gao, J., Li, B., Li, Z., Huang, X. and Wen, G. (2019b), "Synchroextracting chirplet transform for accurate IF estimate and perfect signal reconstruction", *Digit*. *Signal Process*., **93**, 172-186. https://doi.org/10.1016/j.dsp.2019.07.015